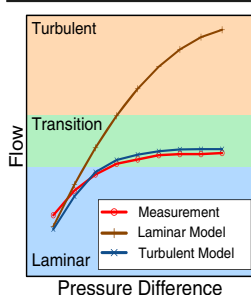


RESEARCH ARTICLE

Gas Flow Dynamics in Inlet Capillaries: Evidence for non Laminar Conditions

Walter Wißdorf, David Müller, Yessica Brachthäuser, Markus Langner, Valerie Derpmann, Sebastian Klopotoski, Christine Polaczek, Hendrik Kersten, Klaus Brockmann, Thorsten Benter

Bergische Universität Wuppertal, Gaußstraße 20, 42119, Wuppertal, Germany



Abstract. In this work, the characteristics of gas flow in inlet capillaries are examined. Such inlet capillaries are widely used as a first flow restriction stage in commercial atmospheric pressure ionization mass spectrometers. Contrary to the common assumption, we consider the gas flow in typical glass inlet capillaries with 0.5 to 0.6 mm inner diameters and lengths about 20 cm as transitional or turbulent. The measured volume flow of the choked turbulent gas stream in such capillaries is $0.8 \text{ L} \cdot \text{min}^{-1}$ to $1.6 \text{ L} \cdot \text{min}^{-1}$ under typical operation conditions, which is in good agreement to theoretically calculated values. Likewise, the change of the volume flow in dependence of the pressure difference along the capillary agrees well with a theoretical model for turbulent conditions as well as with exemplary measurements of the static

pressure inside the capillary channel. However, the results for the volume flow of heated glass and metal inlet capillaries are neither in agreement with turbulent nor with laminar models. The velocity profile of the neutral gas in a quartz capillary with an inner diameter similar to commercial inlet capillaries was experimentally determined with spatially resolved ion transfer time measurements. The determined gas velocity profiles do not contradict the turbulent character of the flow. Finally, inducing disturbances of the gas flow by placing obstacles in the capillary channel is found to not change the flow characteristics significantly. In combination the findings suggest that laminar conditions inside inlet capillaries are not a valid primary explanation for the observed high ion transparency of inlet capillaries under common operation conditions.

Keywords: Inlet capillary, Atmospheric pressure ionization, Capillary flow, Turbulence

Received: 11 February 2016/Revised: 9 April 2016/Accepted: 19 April 2016/Published Online: 31 May 2016

Introduction

Inlet Capillaries in API-MS Systems

In atmospheric pressure ionization mass spectrometry (API-MS) analyte ions generated in an ion source at atmospheric pressure have to be efficiently transferred to the high vacuum region of the mass spectrometer. The initial pressure reduction on this route into the first vacuum region (around 1 mbar to 10 mbar) of the mass spectrometer is typically done by either one of two approaches:

Early API-MS systems were equipped with a small orifice with an inner diameter of approximately $100 \mu\text{m}$ or less [1, 7] between the atmospheric pressure ion source and the first vacuum stage of the instrument. The small diameter of the gas entrance restricted the gas flow into the mass spectrometer significantly, which allowed the pumping system to maintain a comparably low background pressure in the first vacuum stage.

An alternative pressure reduction approach, which is common in modern commercial instruments, is the use of *inlet capillaries* with lengths in the 10 cm to 20 cm range and inner diameters of around 0.11 mm consisting of glass or metal [7, 31, 42]. Due to the flow characteristics in such inlet capillaries, the gas pressure of the bulk gas typically drops to a few hundred mbar along the capillary. This leads to an acceleration of the gas flow in the capillary to trans-sonic conditions [32] followed by an expansion from the capillary end into the first vacuum stage [21]. The primary advantage of inlet capillaries consisting

Electronic supplementary material The online version of this article (doi:10.1007/s13361-016-1415-z) contains supplementary material, which is available to authorized users.

Correspondence to: Walter Wißdorf; e-mail: wissdorf@uni-wuppertal.de

of electrically non conductive material is the option to have a large potential difference across the capillary main axis. Due to the strong viscous drag forces generated by the gas flow, it is possible to transport ions against a potential difference in the 10 kV region [31, 42].

Typically, the transmission efficiency of ions through glass and steel capillaries is in the low percent range but may reach 30% [6, 19, 31]. This considerably high ion transmission is usually explained by the presence of laminar flow inside the capillary duct, which is, therefore, assumed as essential to be maintained. In contrast, the analysis of pipe flow models, which are presented in the following, suggest that the flow through commercially used inlet capillaries is not necessarily laminar under typical conditions. In fact, the flow models suggest at least transitional flow conditions for some common inlet capillaries. In addition, our experimental findings show that in selected inlet capillaries, even substantial modifications of the capillary channel, including the disturbance of the gas flow by obstacles, had no significant effect on the gas throughput and ion transmission efficiency.

We present our experimental findings regarding the nature of the gas flow through typical inlet capillaries of commercial API-MS instruments and compare the results with results from theoretical pipe flow models taken from the literature.

Gas Flows Through Pipes

Inlet capillaries are essentially pipes with an inner diameter in the sub-millimeter range. In the field of fluid dynamics, pipe flow is a classical problem which has been thoroughly investigated since the early stages of research in this area [20, 34, 38].

The gas flow through inlet capillaries is generally of a compressible nature due to the large pressure difference between capillary entrance and exit. It is further considered non adiabatic due to significant heat exchange with the pipe walls and is obviously of a viscous nature which means that friction on the pipe walls has to be taken into account. Nearly isothermal conditions are present because the inlet capillary is not thermally isolated and, in many cases, heated externally. Therefore, any cooling of the gas due to expansion is compensated by heat exchange with the environment.

The pressure loss of the gas flow along the pipe is coupled with an acceleration of the flow (Bernoulli's effect). If the pressure difference along the capillary exceeds a critical ratio, the accelerating flow in the capillary reaches the local speed of sound (the Mach number reaches unity, $Ma = 1$) and, therefore, becomes *transsonic* [8]. Since the flow does not transcend to supersonic conditions in the capillary, the absolute gas mass flow through the capillary is governed by the (limited) maximum flow velocity [36]. In this state, which is referred to as *choked flow*, the flow through the capillary becomes independent from the background pressure at the capillary exit [22, 32, 37].

The emergence of turbulence in pipe flows and the transition from laminar to turbulent conditions in pipes is of particular interest in the literature. Its investigation has a long history [15, 35] but is still an ongoing topic in more recent research [2, 10, 16–18]. Since the turbulence state of the inlet capillary flow is a primary topic of this publication, a brief introduction into turbulence conditions of pipe flows is summarized in the following.

Turbulence Conditions At laminar flow conditions, the flow has no significant velocity components perpendicular to the flow axis, and random disturbances in the flow dissipate quickly due to the viscosity of the flowing fluid. Due to the friction on the capillary walls, a parabolic velocity profile results [20].

Under turbulent conditions, the flow has significant chaotic fluctuations which lead to considerable random velocity components perpendicular to the main flow axis. Chaotic vortices with a wide spectrum of sizes are transported with the flow and interact with each other [10, 17, 20]. This random motion also leads to a considerably increased diffusion of heat and dispersed substances in the bulk gas flow [3, 40]. The pressure loss over the capillary due to Bernoulli's effect is also present in a turbulent flow, but the observed pressure profile differs from the laminar case. Turbulent gas flows have high transverse momentum components, which result in a final velocity profile over the pipe cross-section which is not parabolic and significantly "flatter" than in the laminar case.

A common quantity which allows the estimation of the flow state (turbulent, transitional, laminar) is the *Reynolds number* (Re) [2, 17, 20, 35]. This dimensionless parameter is given by:

$$Re = \frac{\bar{u} \cdot d \cdot \rho}{\eta} \quad (1)$$

Re	Reynolds number
\bar{u}	mean flow velocity
d	diameter of the pipe
ρ	density of the fluid
η	dynamic viscosity of the fluid

Generally, gas flow through a smooth pipe is considered laminar for $Re < 2000$ and turbulent for $Re > 4000$. In the transition region, the flow is generally considered unstable and assumed to potentially shift rapidly to a turbulent state [20, 43]. The dynamics of turbulent transitions and the associated critical Re values for sustained turbulence in pipe flows are active fields of research. Eckhard et al. state that the critical point is very likely to be below 2250 while experimental evidence suggests an even lower value [17]. A more recent thorough study by Avila et al. reports a Re value of about 2040 as a critical value for sustained turbulence [2].

Theoretical Pipe Flow Models There are numerous models in the literature for the description of pipe flow with different assumptions and boundary conditions. In the following, pipe flow models are introduced which are used for comparison with our experimental results.

Volume Flow Models The total gas flow through an inlet capillary is measured with comparably small effort. Thus, models of pipe flow in dependence of external parameters as pressure difference and geometry of the capillary are readily verified with experimental results.

Wutz et al. present equations to calculate the adiabatic compressible volume flow through a long smooth pipe between large gas reservoirs held at given pressures [44]. For laminar conditions, the volume flow Q_{laminar} is calculated as:

$$Q_{\text{laminar}} = \frac{\pi}{128\eta} \cdot \frac{d^4}{l} \cdot \frac{p_0^2 - p_1^2}{2} \cdot \frac{1}{p_0} \quad (2)$$

d inner diameter of the pipe

l pipe length p_0 pressure at the pipe entrance

p_1 background pressure in the downstream recipient

If the flowing fluid is air at a temperature of 20 °C, this simplifies to:

$$Q_{\text{laminar}} = 135 \cdot \frac{d^4}{l} \cdot \frac{p_0^2 - p_1^2}{2} \cdot \frac{1}{p_0} \quad (3)$$

The *turbulent* volume flow $Q_{\text{turbulent}}$ is given by [43]:

$$Q_{\text{turbulent}} = d \left(0.39\pi^2 \cdot \frac{d^3(p_0^2 - p_1^2)}{2l} \right)^{\frac{4}{5}} \cdot \left(\frac{R}{M_{\text{molar}} \cdot T_0} \right)^{\frac{3}{5}} \cdot \left(\frac{4}{\pi \cdot \eta} \right)^{\frac{1}{5}} \cdot \frac{1}{p_0} \quad (4)$$

with the additional quantities:

R universal gas constant

M_{molar} molar mass of the fluid particles

T_0 rest temperature of the inflowing gas

Similarly to the laminar case, this equation is simplified considerably if air at 20 °C is assumed as a flowing fluid:

$$Q_{\text{turbulent}} = 134 \cdot d \cdot \left(\frac{d^3}{l} \cdot \frac{p_0^2 - p_1^2}{2} \right)^{\frac{4}{5}} \cdot \frac{1}{p_0} \quad (5)$$

The term “smooth” in this context stipulates that the wall roughness is below 1% of the pipe diameter, while “long” is also defined by Wutz et al.: For turbulent conditions, the model is valid for a length (l) to diameter (d) ratio of $\frac{l}{d} > 50$. Both requirements are met by glass or drawn metal inlet capillaries.

For the laminar model, the requirements for a pipe to be considered “long” differ:

$$\frac{l}{Q_{\text{laminar}}} > 1.5 \quad (6)$$

This laminar length condition is not fulfilled for some of the inlet capillaries we have investigated; the model authors state that the gas flows will decrease in comparison to the predictions made by Equation 2.

The models by Wutz et al. assume a given turbulence state, either laminar or turbulent, over the whole pressure regime, which represent two limiting cases. A real pipe flow begins in a laminar state with small pressure differences and undercritical exitRe values. With increasing pressure difference, and, therefore, gas velocity, the flow transitions to a turbulent state and, thus, eventually to the volume flow rates as described by the turbulent model.

It should be noted that both models assume adiabatic gas expansion in the capillary. As mentioned earlier, our experimental results show that the flow through the inlet capillaries is, in fact, not adiabatic but nearly isothermal. Fortunately, it was found that in situations where an isothermal flow solution is more appropriate, adiabatic and isothermal solutions converge [32]. Thus, adiabatic models can be used for the description of the flow in inlet capillaries without significant loss of accuracy.

Livesay provides a more sophisticated volume flow model valid for a wide pressure range, which considers also the transition from laminar to turbulent conditions [32]. Since this model is comparably complex and requires the iterative numerical solution of a set of analytically not readily solvable equations, we do not present this model in detail and refer to the original literature [32]. The Livesay model was implemented as a computer program and is used for comparisons with experimental data. It is noted that this model introduces an alternative definition of the Reynolds number:

$$\text{Re} = \frac{4M_{\text{molar}}Q}{RT_0B\eta} \quad (7)$$

with the additional quantities:

B perimeter of the capillary channel

Q gas throughput

Figure 1 depicts the theoretical volume flow for turbulent and laminar conditions in dependence on the capillary exit background pressure while the entrance pressure is held constant. All three models clearly show the effects of choking: with increasing pressure difference (low background pressure at the capillary exit), the increase of the volume flow levels off. If the pressure gradient exceeds a critical ratio (e.g. $\frac{p_1}{p_0} \approx 0.5$ in the turbulent case), the flow becomes almost independent of the pressure difference. The Livesay model, despite its different

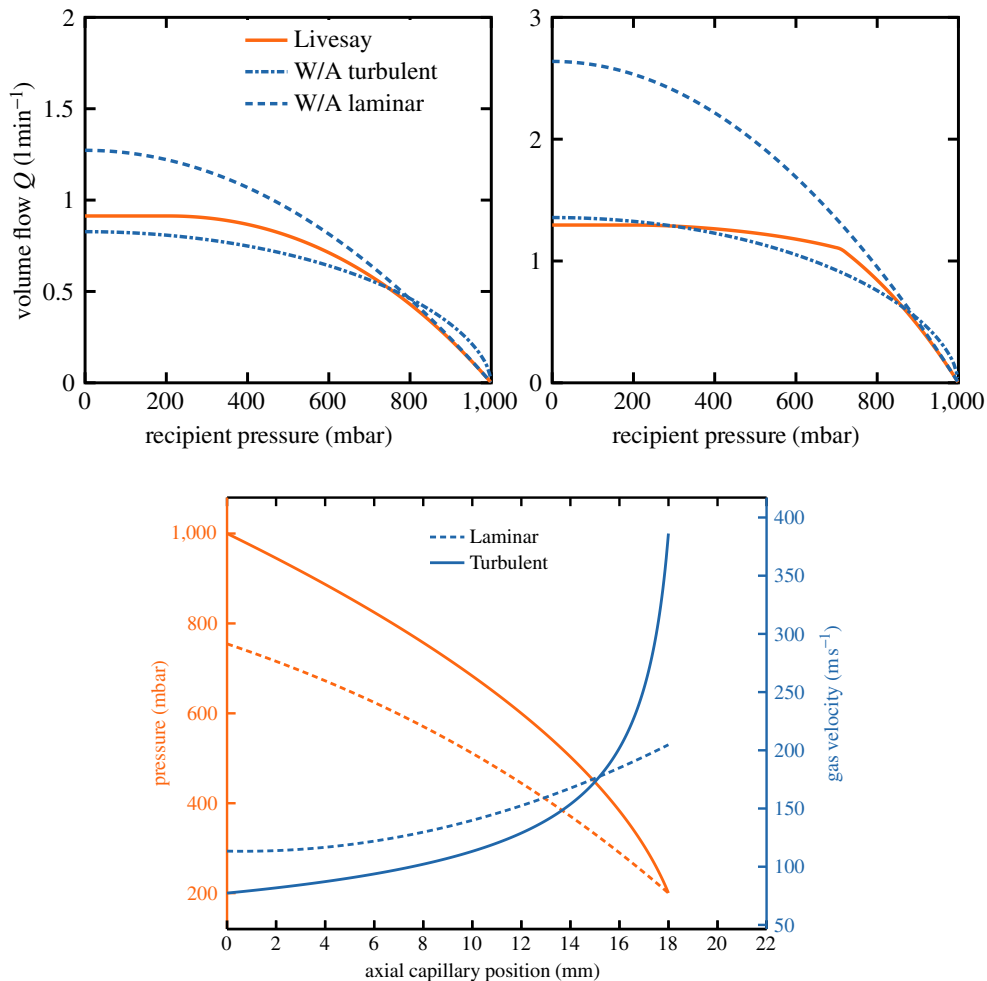


Figure 1. *Top:* Modeled volume flow in dependence on the pressure in the vacuum recipient, calculated with the Wutz/Adam models (Equations 2 and 5) and the Livesay model for two exemplary inlet capillary geometries. The calculated inlet capillary has a length of 18 cm and an inner diameter of 0.5 mm (top left panel) or 0.6 mm (top right panel). The inlet pressure is 1000 mbar. *Bottom:* Modeled velocity and pressure profiles for the turbulent (Michalke) and the laminar model (Venerus). The calculated inlet capillary has a length of 18 cm and an inner diameter of 0.6 mm. The inlet pressure is 1000 mbar, the exit pressure is 200 mbar which is the calculated critical pressure (cf. Equation 12)

modeling approach, converges very well with the laminar Wutz/Adam model for low volume flow rates, while it converges with the turbulent Wutz/Adam model for high-volume flow rates. The change from transitional conditions to fully turbulent choked conditions is observed as a discontinuity in the Livesay model for a capillary diameter of 0.6 mm (cf. right panel in Figure 1).

The turbulent Wutz/Adam model and the Livesay model are directly dependent on the temperature of the in-flowing gas. All three models are also indirectly temperature dependent due to the temperature dependence of the gas viscosity, which is commonly modeled by Sutherland’s law [39]:

$$\eta = \eta_0 \frac{T_0 + C}{T + C} \left(\frac{T}{T_0} \right)^{3/2} \quad (8)$$

T_0 reference temperature (291.15 K)

η_0 reference viscosity at T_0 (18.2 μ Pa·s for air)
 C Sutherland’s constant (120 K for air)

Flow Velocity and Pressure Profile Michalke provides a numerical model of the turbulent compressible gas flow in pipes including heat exchange at the pipe walls [33]. The model yields the one-dimensional velocity profile, which means that the values are averaged over the capillary cross-section. For the turbulent case, corresponding velocities are given by:

$$\frac{c(x)}{c_1} = H(x) \cdot \frac{1}{\sqrt{1 - \frac{(1-p^2) \cdot x}{l}}} \quad (9)$$

$c(x)$ flow velocity at point x
 c_1 flow velocity at the entrance of the pipe
 $H(x)$ Normalized stagnation enthalpy
 P pressure difference entrance/recipient length of the pipe

In this expression, the enthalpy is given as:

$$H(x) = T + (1-T)e^{\frac{x}{l}} \quad (10)$$

$$T = \frac{T_w}{T_k}$$

T_w wall temperature

T_k gas temperature at the inlet

When the gas and wall have the same temperature, the stagnation enthalpy is zero. The one dimensional pressure profile for a turbulent flow is described by:

$$\frac{p(x)}{p_k} = \sqrt{1 - (1-p^2) \cdot \frac{x}{l}} \quad (11)$$

$p(x)$ pressure at point x

p_k pressure at the entrance of the pipe

There is no laminar version of the Michalke model, but Venerus published a numerical perturbation solution for laminar, isothermal compressible pipe flow [41], which yields a two-dimensional axial symmetric solution of the pressure and velocity fields in the capillary. This model is, again, rather complex; thus, the reader is referred to the original publication [41]. Similar to the Livesay model for the pipe volume flow, the Venerus model was implemented as a computer program. It should be noted that in the model by Venerus, the mass flow rate is an input parameter, which, in turn, has to be calculated from a different model or determined experimentally. Figure 1 presents the laminar and turbulent flow model in comparison. The laminar flow rate was calculated using the laminar model by Wutz/Adam (Equation 2), the turbulent case results from the turbulent Wutz/Adam model (Equation 4)

Assumption of Laminar Conditions in Inlet Capillaries

A common notion in the mass spectrometry community is that the flow in inlet capillaries is laminar. This is inferred from the assumption that ions colliding with the capillary wall are discharged and thus lost and contradicting the general observation of high ion transport efficiencies of inlet capillaries [31; Whitehouse, Personal Communication]. Exemplary calculations for two commercial inlet capillary geometries (length 18 cm, inner diameters 0.5 mm and 0.6 mm) do not clarify the situation. If the Reynolds number in the capillary is estimated by calculating the mean density and mean flow velocity from the laminar and turbulent flow models by Venerus and Michalke, an ambiguous result emerges as presented in Table 1. Depending on the chosen flow model and the inner capillary diameter, the estimated Reynolds number is either in the fully laminar region, transitional or even in the region considered as fully turbulent. In the case of the 0.6 mm capillary, both flow models predict transitional or even turbulent conditions. Thus, the general assumption of laminarity in inlet capillaries is contradicted by the mentioned models of gas flow through pipes.

Table 1. Flow Parameter Calculation Results for Two Exemplary Inlet Capillary Diameters

	0.5 mm	0.6 mm
Michalke model:		
Mean turbulent flow velocity \bar{u}_t (m·s ⁻¹)	113.6	129.4
Mean turbulent pressure \bar{p}_t (mbar)	688.5	688.5
turbulent Re	2651	3624
Venerus model:		
Mean laminar flow velocity \bar{u}_l (m·s ⁻¹)	117.7	142.7
Mean laminar pressure \bar{p}_l (mbar)	449.7	520.0
laminar Re	1784	3020

The calculated inlet capillaries have a length of 18 cm. The inlet pressure is 1000 mbar; the exit background pressure is 200 mbar

Additionally, there is experimental evidence which contradicts the assumption of an undisturbed, laminar flow in inlet capillaries. Recently, ionization and sampling methods have been developed which involve the modification of inlet capillaries and result in significant disturbances of the gas flow [12, 13, 23, 27]. A very likely consequence of such a disturbed flow in an over-critical, transitional flow regime is the induction of flow fluctuations which do not disappear below a Re value larger than approximately 2250 [17], but rather lead to turbulent flow conditions. However, even in this presumably unfavorable situation, the ion transfer characteristics of the modified inlet capillaries remained high and, generally, no significant loss of transmission efficiency was reported by the developers of those methods. This supports the notion that ions are efficiently transported even in turbulent flow through an inlet capillary.

To our knowledge there is currently no investigation on the gas flow of common inlet capillaries that clearly verifies the generally assumed laminar flow conditions. In this work, we present our investigations of the gas flow in inlet capillaries commonly used in commercial mass spectrometers. The results obtained, in fact, support the notion of at least *transitional* if not *turbulent* flow conditions for a number of the examined capillaries.

Experimental

Overview

To investigate the flow conditions, four sets of experiments were conducted with a selection of glass and metal inlet capillaries of different geometrical shape:

1. *Volume flow measurements:* The volume flow through inlet capillaries was measured in dependence of the downstream background pressure, the geometrical shape of the capillary and the capillary temperature, respectively.
2. *Pressure gradient measurements:* The duct of glass inlet capillaries was partly opened and the static pressure at

particular positions along the capillary channel was measured.

3. *Temperature measurements*: The outflow temperatures of gas exiting a heated inlet capillary was measured, which allowed the investigation of the extent of the heat exchange of the gas with the capillary walls.
4. *Ion transfer times*: The transfer times of ions generated within quartz inlet capillaries by laser photoionization were measured. This allowed the direct investigation of the gas velocities in the inlet capillary, utilizing photoions as tracing particles.

The details of the individual experimental setups and the used capillaries are described below.

Capillary Types

Experiments were conducted with custom borosilicate glass and metal capillaries. The glass capillaries had inner diameters of 0.5 mm or 0.6 mm and lengths in the 10 cm to 22 cm range, which resemble commercially available inlet capillaries used in Bruker Daltonics (Bremen, Germany) and Agilent (Santa Clara, CA, USA) API-MS instruments. The capillaries were made from bulk stock material, purchased from Hilgenberg GmbH (Malsfeld, Germany). Approximately 2 cm of each end of the capillary were electrochemically metalized allowing application of electrical potentials to these regions (unless otherwise stated).

Some of the glass capillaries were modified individually for selected experiments, e.g. by drilling perpendicular channels through the capillary wall for static pressure measurements. Those modifications are presented in detail in the sections for the individual experiments.

Stainless steel capillaries similar to the inlet capillaries used in Thermo Fisher Scientific instruments (Bremen, Germany) were obtained from Ziemer Chromatographie (Klaus Ziemer GmbH, Langerwehe, Germany). These metal capillaries had inner diameters of 0.2, 0.5 and 0.75 mm and lengths of 10 cm to 22 cm, and were left unmodified.

Volume Flow Measurements

The basic experimental setup used for investigations of the volume flow through inlet capillaries was based on a custom vacuum recipient equipped with a rotary vane pump (80 m³/h, Duo 060A, Pfeiffer Vacuum GmbH, Asslar, Germany). The pumping speed was adjusted with a pressure-regulated butterfly valve (MKS 252 exhaust valve controlled by a MKS 252E exhaust controller, MKS Instruments GmbH, München, Germany) which allowed the automatic stabilization of a selected background pressure in the recipient. The recipient pressure was measured with two Baratron absolute pressure transducers covering the entire pressure range (Barocel 600A–1000 T, Datametrics/Dresser, Wilmington, MA, USA) and more accurately the 0 mbar to 10 mbar range (122AAX–00010DBS, MKS Instruments GmbH, München, Germany). This setup

was used to select a regulated background pressure in the range of 1 mbar to 1000 mbar.

The inlet capillaries were attached to the vacuum recipient by a custom flange. A laminar flow ion source (LFIS), introduced by Barnes et al. [4, 23, 25], or a custom ionization chamber were mounted upstream of the inlet capillary. The volume flow through the inlet capillary was measured by a drum type gas flow meter (TG05, Ritter Apparatebau GmbH and Co. KG, Bochum, Germany), which was attached to the entrance of the capillary. The utilized gas flow meter measures the absolute gas flow with a rotating cylinder drum which imposes only a negligible pressure drop in the measurement instrument (≈ 0.4 mbar). Alternatively, mass flow controllers of different ranges (Mass-Flo-Controller; MKS Instruments, Andover, MA, USA) were used for flow measurements. Additionally, these controllers were used to restrict the absolute gas flow in experiments that required controlled volume flows. The accuracy of the pressure difference measurement is well below 1%. Due to the fact that the drum gas meter was not used in a temperature-controlled environment, the accuracy of the flow measurements is estimated to be around 1% even if the flow meter has a much better stated accuracy.

Figure 2 is a schematic showing the experimental setup (including the arrangements for ion transfer time measurement described in the following).

Temperature Variation

Volume flows were measured under variation of the capillary temperature. Metal capillaries were directly resistively heated. The glass capillaries were heated using a tantalum wire coil covering the entire glass body. The stated temperatures were the temperatures measured with thermocouples mounted on the capillary outer wall. It was shown in previous studies that the gas temperature inside the capillary readily adjusts to the measured temperature of the outer capillary surface [29].

To further investigate the heat transfer from the capillary walls into the gas stream, short segments of the capillary were heated in a similar fashion close to the downstream exit port of the capillary.

Pressure Measurements in Capillaries

For pressure measurements within the capillary channel, small holes (diameter approx. 0.1 mm) were drilled into the glass capillary wall at different axial positions. The local static pressure was measured using a Bourdon tube gauge with the required pressure range.

Ion Transfer Time Measurement

For ion transfer time measurements the glass inlet capillary was replaced with a silica capillary (Hilgenberg GmbH; Malsfeld, Germany) of 18 cm length and an inner diameter of 0.4 mm. Ions were generated by atmospheric pressure laser ionization (APLI) [5, 9] directly in the capillary duct. A KrF* excimer laser (248 nm; ATLEX300, ATL Lasertechnik, Wermelskirchen,

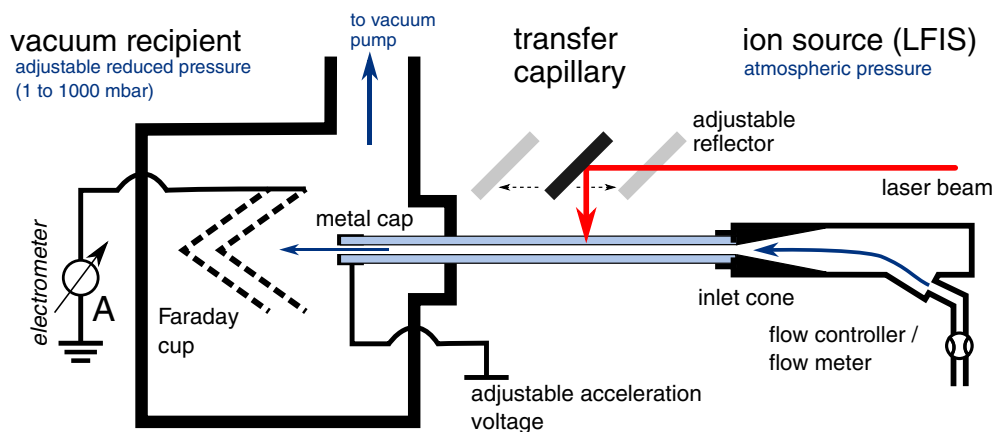


Figure 2. Schematic of the transfer time measurement setup, consisting of vacuum recipient with ion current measurement devices and inlet capillary. The glass or metal inlet capillary are heatable. Utilization of a quartz capillary allows laser ionization inside the inlet capillary

Germany) was used as light source and toluene was used as an analyte. A constant toluene mixing ratio of 3%V was obtained by mixing the head space of liquid toluene held at room temperature with the primary N_2 gasstream. The ion current was measured inside the vacuum recipient with a Faraday cup, which was connected to an amperemeter (Keithley Instruments 610C, Cleveland, OH, USA) [28].

Temporally resolved ion current measurements were performed by connecting the amplifier output of the ampere meter directly to a digital oscilloscope (TDS 1012, Tektronix Inc., Beaverton, OR, USA). The oscilloscope was triggered by the trigger output reference signal of the ionizing laser. Thus, the ionizing laser pulse served as starting point for the presented ion transfer time measurements. Figure 2 depicts the measurement setup schematically.

Chemicals

Nitrogen and synthetic air were purchased from Gase.de, Sulzbach, Germany, with a stated purity of 99.999%vol. Toluene was obtained from Sigma-Aldrich GmbH (Seelze, Germany) in the highest purity available and was used without further purification.

Numerical Calculations

Numerical calculations were performed to estimate the loss of tracer ions in an inlet capillary assuming a laminar gas flow and complete destruction of ions on the capillary walls. Further, the heat transfer from the capillary walls into an assumed laminar gas flow was simulated to investigate whether or not the experimentally determined temperatures of the gas exiting the capillary are in accord with the assumption of a laminar gas flow in the capillary.

The depletion of hypothetical tracer ions and the temperature distribution in the capillary gas flow was numerically estimated with Comsol Multiphysics (version 4.4, Comsol

AB, Stockholm, Sweden). A defined velocity distribution derived from the Venerus model for laminar compressible tube flow [41] was used. It has a parabolic velocity cross-section, the velocity on the wall is zero (no slip condition) and the maximum flow velocity is reached on the center axis of the capillary. The resulting flow field was used for a convection/diffusion calculation using the "transport of diluted species" module of Comsol. The diffusion coefficient of the simulated analyte was varied to estimate the extent of depletion of analyte ions with different molecular masses. On the inner capillary walls, an ion concentration of zero was assumed, which corresponds to an assumed complete destruction of the tracer on the capillary walls. The tracer molecules were assumed to be electrically neutral and no electrokinetic migration was considered in the calculations. This approach estimates a lower limit for diffusional losses on the capillary walls, since the additional electric force would increase the radial transport to neutral capillary walls.

The "heat transfer in fluids" module of Comsol was used to simulate the temperature distribution in the gas flow as predicted by the laminar flow model. The flow field of the Venerus model was also used as a base for this calculation. According to performed experiments, the capillary wall in a segment of 2 cm length at the end of the capillary was heated to 353 K while the remaining capillary and the inflowing gas was assumed to be at room temperature (298 K). The simulated fluid was nitrogen in both models. All gas parameters (e.g. heat capacity, heat conductivity) were taken from the Comsol material library.

The flow models by Venerus and Livesay were implemented as computer programs in the Python programming language, utilizing the numerical and visualization libraries of NumPy¹ and Matplotlib.²

¹<http://www.numpy.org>

²<http://matplotlib.org>

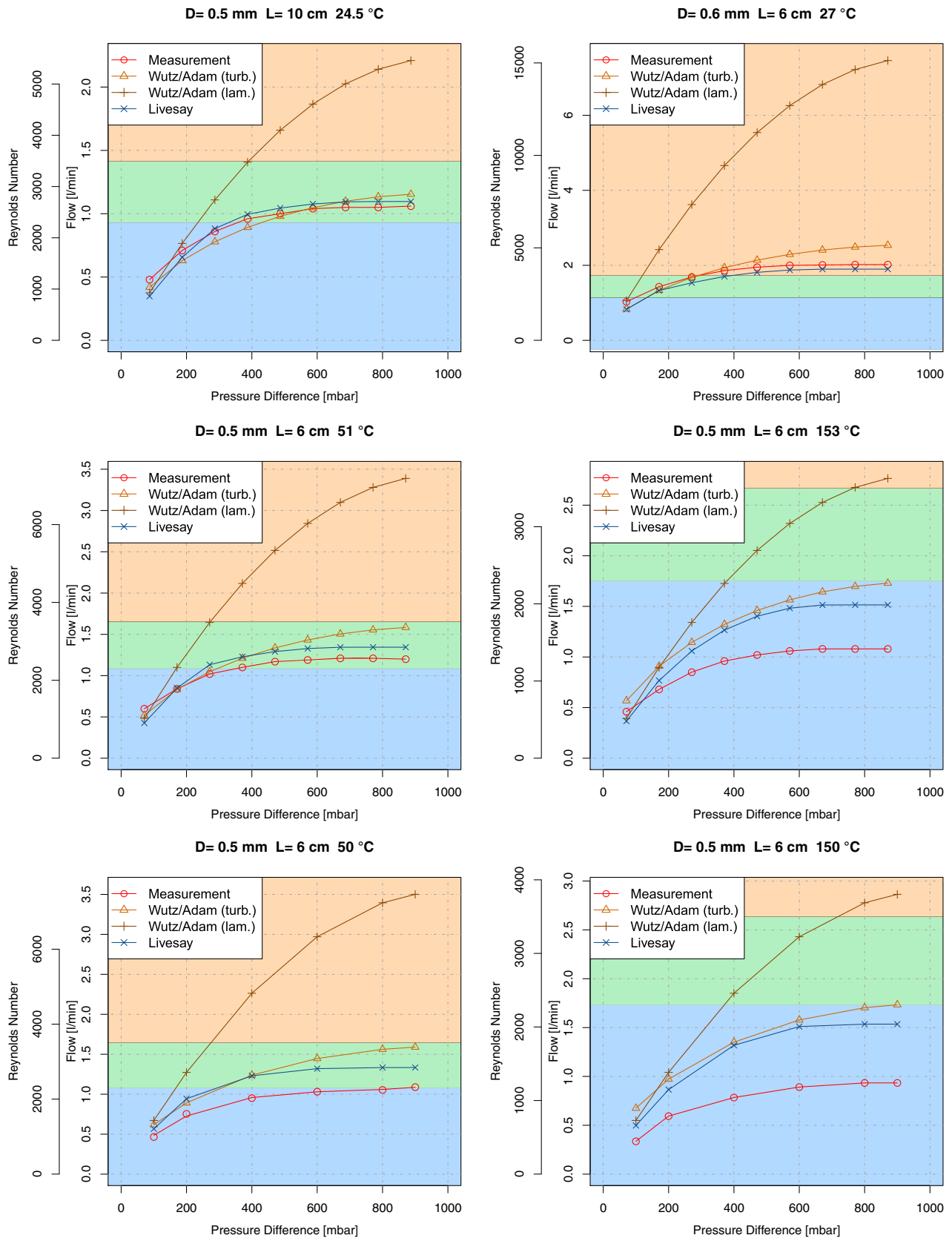


Figure 3. Volume flow through selected glass (top and center) and metal (bottom) inlet capillaries at room and elevated temperature in comparison to theoretical flow models. The inlet pressure was 1000 mbar. The flow regimes are marked by the background colors. Blue: laminar ($Re < 2300$), green: transitional ($2300 < Re < 3500$), red: turbulent ($Re > 3500$). Re values calculated with Equation 7

Results

Temperature-Dependent Volume Flow

The gas flow through glass and metal inlet capillaries of different geometries was measured under variation of the capillary temperature. Figure 3 presents typical results of the volume flow through glass capillaries in dependence of the background pressure in the vacuum recipient at room temperature. The volume flow increases with decreasing background pressure until the flow in the capillary becomes choked at a pressure difference of approximately 500 mbar. Here, the volume flow becomes almost independent from the background pressure. Typical operational conditions of an inlet capillary in an actual API instrument would be a pressure difference of at least 900 mbar between the capillary entrance and exit. Thus, the flow through an inlet capillary attached to an API instrument under operational conditions is, as is well known, fully choked.

The capillary geometry is necessarily strongly affecting the volume flow, as with increasing capillary diameter the volume flow increases rapidly while with increasing length of the capillary the volume flow decreases. This is demonstrated in Figure 3: by increasing the inner diameter from 0.5 mm to 0.6 mm and shortening the capillary from 10 cm to 6 cm, the volume flow doubles. The two exemplary results in Figure 3 at room temperature also clearly show that in selected inlet capillary configurations, the flow through the capillary is transitional or even turbulent, with the Reynolds numbers well above 3500.

This notion is supported by experiments in which artificial disturbances of the flow were induced by placing a small obstacle inside the capillary channel. An overcritical gas flow would become readily turbulent if it was not already in a turbulent state. In the experiments, the volume flows that were measured for overcritically operated capillaries with and without an obstacle were identical, which strongly suggests the presence of an already turbulent gas flow.

Both the turbulent flow model by Wutz/Adam and the flow model by Livesay describe the experimentally determined volume flow at room temperature comparably well. In direct comparison, the Wutz/Adam model has a larger divergence from the experimental values than the Livesay model. This finding was consistently observed for other capillary geometries under room temperature conditions (cf. the [supplemental material](#) for details). In contrast, the laminar Wutz/Adam model predicts a volume flow, which is generally significantly too high; the predicted values are at least a factor of two higher than the experimental results.

Figure 3 also presents the volume flow through glass and metal capillaries at elevated temperature. The comparison between the capillary types shows that the volume flow is independent of the capillary material: the measured volume flow differs only slightly between glass and metal capillaries. Detailed analysis of the results from all performed experiments with different capillary geometries and measurement temperatures show that the observed differences in Figure 3 are in the

range of geometrical experimental uncertainties between individual capillaries (see [supplemental materials](#) for details). Such individual differences are likely induced by deviations of the capillary diameter from the manufacturers stated value. Thus, flow characteristics are similar for the investigated glass and metal capillaries within a temperature range of 20 to 50 °C. Therefore, parameters like wall roughness or wall friction, which potentially differ between glass and metal capillaries, have only a negligible influence on the volume flow in the present experiments.

Increasing the capillary temperature has, again, a significant effect on the volume flow, as expected. As shown in Figure 3, the flow decreases with increasing temperature. This effect is also shown in Figure 4: the volume flow at the lowest attainable recipient pressure linearly decreases with increasing temperature. Figure 3 shows another interesting effect of the increasing temperature: the Reynolds numbers decrease significantly due to the increasing viscosity and the decreasing density of the gas. Consequently, Re drops rapidly to undercritical values and the predictions of the flow should become laminar.

The experimentally determined volume flow and the flow models diverge with increasing capillary temperature, which is clearly observed in Figure 4. Additionally, the turbulent Wutz/Adam and Livesay flow models do not even describe the direction of change in the flow in dependence of the capillary temperature correctly. Under specific conditions, both models predict increasing gas flow with increasing temperature, while the experimentally determined volume flow actually declines. In the case of the flow model by Livesay, such an increasing divergence is expected, since the boundary conditions of this model are violated at an elevated capillary temperature. The model is explicitly temperature-dependent and assumes hot gas entering the flow duct. In the performed experiments, the gas entering the heated capillary was at room temperature and then heated within the capillary duct by heat exchange with the capillary walls. Similarly, a divergence between the Wutz/Adam model and the experimental results with increasing temperature is also not surprising due to the fact that the basic assumption of isothermal flow conditions, which transforms to nearly adiabatic conditions in the case of the capillary, is violated in the experiments. Further investigations with preheated gas entering the capillary will reveal if the increasing temperature difference between capillary walls and inflowing gas is the primary reason for the divergence between the flow models and the experimental results.

Static Pressure

The static pressure was determined on different positions along glass inlet capillaries with 0.5 mm and 0.6 mm inner diameters at minimum attainable backing pressure in the recipient. The inlet pressure was approximately 1000 mbar; the exit background pressure was approximately 2.5 mbar. To calculate the

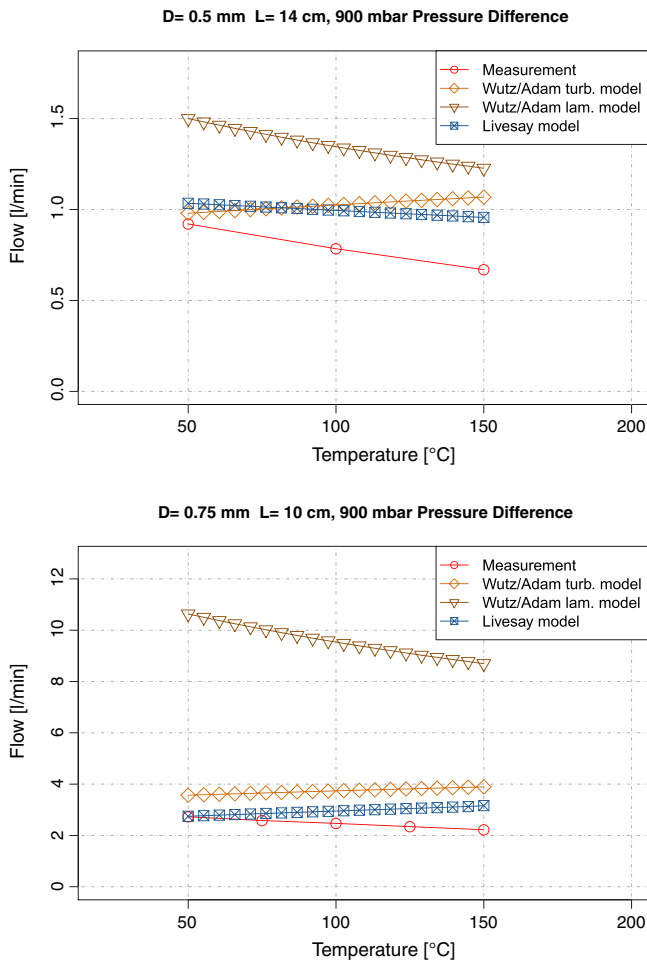


Figure 4. Experimental temperature dependence of volume flow through metal capillaries in comparison to results from flow models

pressure profile along the capillary with the models by Michalke and Venerus, the exit plane pressure of the capillary has to be estimated. Due to the choked flow conditions, the exit pressure is significantly higher than the background pressure in the vacuum recipient. Wutz et al. provide an equation which allows the calculation of the critical pressure at which the flow in the capillary becomes sonic and, thus, chokes [44]. This critical pressure is also the capillary exit pressure for a choked flow. For air under turbulent conditions at room temperature, the critical pressure p_c is given by (with d and l in cm and p_0 in mbar):

$$p_c = \frac{4.51 \left(\frac{d^3 p_0^2}{2l} \right)^{\frac{4}{7}}}{d} \quad (12)$$

Table 2 summarizes the results of the measurements and calculations. The measured static pressures are in agreement with the calculated turbulent static pressures with a deviation in the range of $\pm 6\%$ while the calculated laminar pressures deviate strongly in all cases.

Table 2. Static Pressure Measurements in Glass Inlet Capillaries

Capillary	1	2	3
Cap. diameter (mm)	0.6	0.6	0.5
Position (cm)	15.3	17.4	9.0
Meas. Volume flow ($L \cdot \text{min}^{-1}$)	1.37	1.16	0.907
Calculated critical pressure (mbar)	209	207	186
Calculated turbulent static pressure (mbar)	439	274	727
Calculated laminar static pressure (mbar)	250	216	352
Measured static pressure (mbar)	460	290	720

Gas Temperature

Direct measurements of the gas temperature expanding from heated inlet capillaries show that the flow within the capillary duct is nearly isothermal with extensive heat exchange between the capillary walls and the gas. Table 3 presents the measurement results. A heated capillary segment of only 2.0 cm at the capillary end is sufficient to heat the flowing gas to almost the temperature measured at the heating coil on the outer capillary walls. As an analogy, if a 2.0 cm segment is heated at the center of the capillary main axis, the gas is almost returned back to ambient temperature when it exits the capillary. Both findings indicate extensive heat exchange with the capillary walls, which supports the general notion of transient or turbulent conditions due to an increased turbulent heat transport in the gas.

The estimated temperature distribution in a hypothetical laminar gas flow through the capillary was calculated with Comsol Multiphysics. The gas flow and pressure fields were calculated from the laminar flow model by Venerus and a heated segment of 2.0 cm at the capillary exit with a temperature of 354 K was assumed. Figure 5 presents the radial temperature distributions at the capillary exit for different hypothetical volume flows Q . The results are not entirely conclusive: for a volume flow of $Q = 1.0 L \cdot \text{min}^{-1}$, which corresponds to the actually measured flow conditions in the inlet capillary with the simulated geometry, a temperature profile with a mean temperature of 344 K results. Thus, the simulated mean exit temperature for a hypothetical laminar case is 10 K below the temperature of the heated capillary walls. In the experiment, a temperature difference of only 5 K was found which also supports the notion of increased heat exchange due to turbulent mixing. Given the uncertainties of the numerical model and the

Table 3. Gas Temperature Measurements on a Glass Inlet Capillary with 0.5-mm Inner Diameter and 18-cm Length

Heated segment (cm)	Cap. temp. (°C)	Expanding gas temp. (°C)	Recipient pres. (mbar)
9–18	70	63	4
9–15.5	65	49	4
0–18	80	75	8
8–11	65	29	4
15.5–18	55	52	4
15.5–18	80	75	3

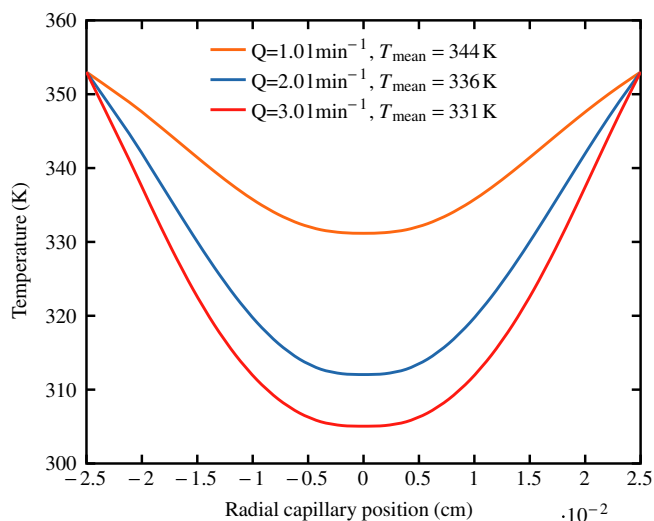


Figure 5. Calculation of the radial temperature distribution at the exit plane of a capillary with a 0.5 mm inner diameter and a heated capillary segment (354 K) of 2.5 cm at the exit for different volume flows Q . The flow field in the capillary was calculated from the laminar flow model. The mean temperature was calculated by scaling the temperatures on the radial profile with the local circumference

experiments, this difference is not a particularly strong indication of turbulent conditions. However, it is consistent with the assumption of transient or turbulent conditions in the investigated capillaries.

Velocity Profile

By generating ions with photoionization using a pulsed ns UV laser [atmospheric pressure laser ionization (APLI)] in a quartz capillary and recording the transfer time from the ionization position to a Faraday cup detector or a detector electrode, the gas flow profile along the capillary channel is experimentally determined. The results of such time of flight (ToF) measurements yield the profile of the flow velocity in the remaining capillary segment between the point of ionization and detector.

Figure 6 shows the ToF results performed on a quartz capillary with an inner diameter of 0.4 mm and a length of 18 cm with a minimum attainable pressure in the recipient. The Reynolds number of this setup is calculated to be 1449 with the laminar flow model and 1733 with the turbulent flow model. Thus, the capillary flow in this setup is considered as *laminar*. Experiments with capillary geometries which should lead to a turbulent flow are planned but were not conducted to date due to the lack of available quartz capillaries with appropriate geometric parameters.

With the exception of a few outlying individual data points near the capillary exit where the transfer times become very short and the limits of the used experimental setup are reached, the measurement results show a smooth and reproducible ion velocity distribution along the capillary. It is noted that in the experiments the initial rise of the transient signal of the ion pulse was recorded, not the average transfer time of the

transported ions. Thus, the experiment yields the velocity of the fastest ions, which are transported in the center region of the capillary flow, not the radially averaged flow velocity. This maximum ion velocity is in the range of 150 to 200 $\text{m}\cdot\text{s}^{-1}$.

The experimental data are compared with results from calculations with the turbulent and laminar flow models by Michalke and Venerus. Figure 6 shows that the averaged flow profiles diverge significantly from the experimental results. This is expected due to the detection mode in the experiments.

Therefore, the resulting ion pulses resulting from a laser-induced start zone of 5 mm axial length were simulated in a numerical model with Comsol Multiphysics. In the laminar version of this model, the two-dimensional compressible laminar flow model from Venerus was used to calculate the background gas flow for the convection/diffusion simulation. In the turbulent case, a two-dimensional flow profile was estimated by calculating the one-dimensional average flow velocity by the flow model of Michalke and then assuming a parabolic radial flow profile. For the determination of the minimal simulated ion transfer time, the initial rise of the simulated ion pulses was determined from the simulation results.

The comparison of the experimental results with the ion transport simulation reveals that the laminar transport model reproduces the experimental data. In contrast, the turbulent transport model results diverge significantly from the experiments as expected. This strongly suggests that the flow in the quartz capillary was in a laminar state, as expected from the calculated Reynolds number, and that the laminar flow model describes the laminar compressible flow correctly.

Planned further experiments with over-critically operated capillaries will show whether or not the turbulent model is reproducing the velocity profile of a fully turbulent capillary flow as well.

Ion Transmission Efficiency Through Inlet Capillaries

Measured ion transmission efficiencies of inlet capillaries made of glass are surprisingly high; the ion loss was measured to be smaller than one order of magnitude for gas flows containing ions of both polarities [6]. A detailed publication regarding the transmission of small gas phase ions through metal and glass inlet capillaries is currently in preparation. It is widely assumed that this high ion transmission is due to a laminar flow inside the inlet capillary, as ions that collide with the wall are assumed to be discharged [31]. However, within inlet capillaries operated at typical API conditions, a high fraction of the ions do reach the capillary walls during their passage due to molecular diffusion, even if a strictly laminar flow through the capillary duct is assumed. For turbulent gas flows, the transverse transport of ions by turbulent diffusion is orders of magnitudes larger than the molecular diffusion [14, 40]. Therefore, the following calculation yields only a lower limit for the diffusion in this case. In addition to molecular diffusion, space charge can influence the ion motion and potentially contributes to the drag towards the capillary wall [31]. While space charge effects

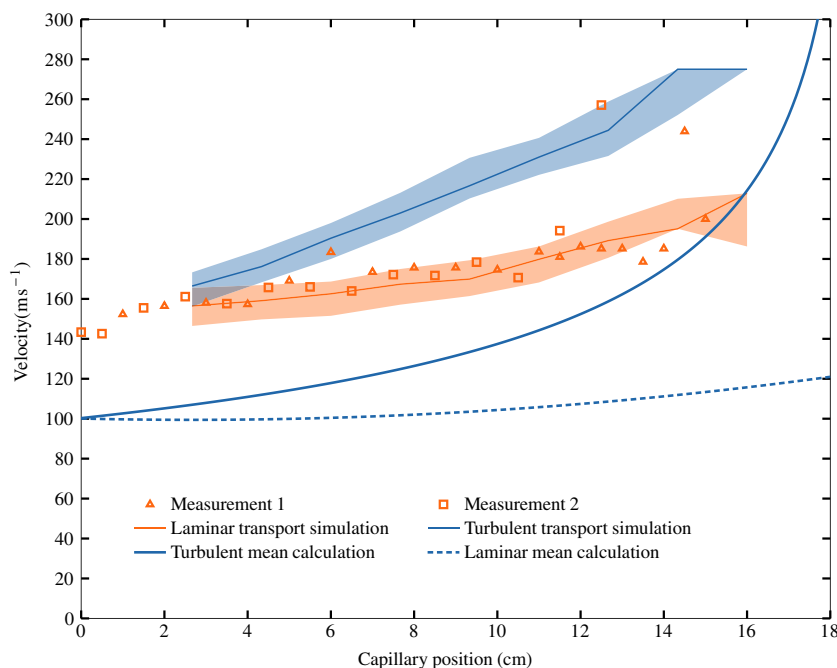


Figure 6. Flow profile along an inlet capillary with an inner diameter of 0.4 mm and a length of 18 cm. The measured velocity results from the leading edge of the ion pulse started at the ionization position which corresponds to the first ions reaching the detector. The theoretical mean velocity profiles were calculated from the turbulent flow model by Michalke et al. and the laminar model by Venerus. The ion transport simulation results were determined from a numerical convection / diffusion model of the ion transport in the capillary. The uncertainty of the numerical model resulting from a variation of the signal threshold which is considered as starting point of the ion pulse is indicated in the colored bands

are not easily calculated, the transport velocity of the molecular diffusion is described by the Einstein–Smoluchowski relation [30]. The mean distance a molecule is transported by diffusion is given by:

$$x = \sqrt{2 \cdot D \cdot t} \quad (13)$$

with:

x distance of diffusion

D diffusion coefficient

t time

The diffusion coefficient depends on pressure and temperature. In most cases, the inlet capillary has a specific temperature without a significant axial temperature gradient, but the pressure decreases along the main capillary axis. For a rough estimation of a diffusion coefficient, a mean pressure of 500 mbar is assumed (refer to the pressure profiles in Figure 1). The diffusion coefficient is calculated using the following equation:

$$D = \frac{1}{3} \cdot \lambda \cdot \bar{v} \quad (14)$$

with:

λ mean molecular free path

\bar{v} mean molecular velocity

When ions with a molecular weight of $30 \text{ g}\cdot\text{mol}^{-1}$, a mean velocity of $460 \text{ m}\cdot\text{s}^{-1}$ and a mean free path of 200 nm are assumed, a diffusion coefficient of $0.303 \text{ cm}^2\cdot\text{s}^{-1}$ is obtained. Most typical analyte ions traveling through inlet capillaries have a considerably larger molecular diameter than nitrogen, so that their diffusion coefficients are much smaller. Assuming an inlet capillary with a length of 18 cm and an inner diameter of 0.5 mm, the transfer time from the entrance to the exit of the capillary is around 1.3 ms [23]. Equation 13 gives an average diffusion distance of 0.3 mm for each molecule. Therefore, even small gas phase molecules, which enter the capillary at the center capillary axis, reach the capillary wall entirely driven by molecular diffusion.

This simple calculation is supported by a numerical model: a diffusion and convection calculation to simulate the analyte depletion within the inlet capillary duct was carried out, assuming a generic analyte and a complete destruction of the analyte ions hitting the capillary walls. Figure S1 in the supplemental materials shows the extent of analyte depletion for different diffusion coefficients. The simulation shows that for very small molecular weight analytes, a nearly complete destruction is estimated even in a laminar bulk gas flow. As stated before, these calculations define a lower limit of collisions with the walls and do not take any additional mixing processes into account. Thus, a laminar flow within the capillary duct is not considered as the primary explanation for the observed high ion transmission of inlet capillaries. Other mechanisms which

potentially lead to high transmission efficiencies are surface effects, e.g. charging of the capillary walls.

Conclusions

The investigation of the gas flow through inlet capillaries typically used as a first gas flow restriction stage in atmospheric pressure mass spectrometers reveals the high complexity of the flow characteristics. Commonly used inlet capillaries can be in the laminar, transitional and turbulent region, depending on the particular capillary geometry and operational conditions. This renders the experimental determination of the actual flow state rather complex, particularly if the flow is of a transitional type.

For the investigated commercially used inlet capillary geometries with 0.5 and 0.6 mm inner diameters, the flow is at least in the transitional region. Volume flow measurements and the direct measurements of the static pressure strongly support the presence of a turbulent gas flow. The theoretical turbulent models are in agreement with the experimental results for room temperature. Additionally, the placement of an obstacle in a capillary duct did not change the volume flow significantly, which suggests that even the undisturbed flow in the investigated capillary was already turbulent. The measured extensive heat exchange with the capillary walls does further support the assumption of a turbulent gas flow. In contrast, the experimental findings are generally in conflict with the assumption of a laminar flow: the numerical simulation of the ion depletion in a hypothetical laminar gas flow supports the assumption that laminarity is not a prerequisite for high ion transmission efficiencies. Even under laminar conditions, the ion loss is severe assuming ideal ion destruction on the capillary walls. Such a behavior was not found in preliminary ion transmission measurements. Thus, it is concluded within the framework of this paper that ions are not generally discharged on the capillary walls but participate in a potentially complex surface–gas phase exchange chemistry on the walls. In the investigated cases, the capillary material had no significant effect on the flow dynamics: The measured flows through the metal capillaries are similar to the results gathered on glass capillaries and, therefore, also to the theoretical predictions.

Experiments with heated capillaries clearly show that the theoretical models become invalid with increasing capillary temperature, which is partly expected due to the increasing violation of particular boundary conditions of the models. Further experiments, in particular with pre-heated gas flowing through the inlet capillary, will show if the flow models also hold true under increased temperature if the model assumptions are satisfied.

The experimentally determined velocity profile in a laminar capillary flow was reproduced by a numerical model based on the laminar flow model by Venerus. Further experiments will reveal if this is also the case for turbulent conditions and the corresponding turbulent flow model.

The generally present turbulent flow through the investigated inlet capillaries allows significant modification of the

capillary duct without altering the flow characteristics. This opens the way to ionization inside the inlet capillary: different ionization methods have already been carried out inside the capillary duct; these are photoionization (capillary atmospheric pressure photoionization, cAPPI [23, 24, 26]), laser ionization (capillary atmospheric pressure laser ionization, cAPLI [28]) and, in the negative ionization mode, electron capture ionization (capillary atmospheric pressure electron capture ionization, cAPECI [11, 12]). With the necessity of laminar flow conditions in the capillary, the options of interesting methods involving the inlet capillary would be very limited, which is apparently not the case.

References

- Anderson, J.B., Andres, R.P., Fenn, J.B.: Advances in Atomic and Molecular Physics. In: Bates, D.R., Estermann, I. (eds.) *Advances in Atomic and Molecular Physics*. Academic Press, New York (1965)
- Avila, K., Moxey, D., de Lozar, A., Avila, M., Barkley, D., Hof, B.: The onset of turbulence in pipe flow. *Science (New York, N.Y.)* **333**(6039), 192–196 (2011)
- Baldwin, L.V., Walsh, T.J.: Turbulent diffusion in the core of fully developed pipe flow. *AIChE J.* **7**(1), 53–61 (1961)
- Barnes, I., Kersten, H., Wißdorf, W., Pöhler, T., Hönen, H., Klee, S., Brockmann, K.J., Benter, T.: Novel Laminar Flow Ion Source for LC- and GC-API MS. Proceedings of the 58th ASMS Conference on Mass Spectrometry and Allied Topics, Salt Lake City (2010)
- Benter, T.: Atmospheric Pressure Laser Ionization MS. In: Gross, M., Caprioli, R.M. (eds.) *The Encyclopedia of Mass Spectrometry Volume 6: Molecular Ionization Methods*. Elsevier Science, Oxford (2007)
- Brockmann, K.J., Wißdorf, W., Hyzak, L., Kersten, H., Müller, D., Brachthäuser, Y., Benter, T.: Fundamental Characterization of Ion Transfer Capillaries Used in Atmospheric Pressure Ionization Sources. Proceedings of the 58th ASMS Conference on Mass Spectrometry and Allied Topics, Salt Lake City (2010)
- Bruins, A.P.: Mass spectrometry with ion sources operating at atmospheric pressure. *Mass Spectrom. Rev.* **10**(1), 53–77 (1991)
- Chivers, T.C., Mitchell, L.A.: On the limiting velocity through parallel bore tubes. *J. Phys. D Appl. Phys.* **4**(8), 303 (1971)
- Constapel, M., Schellenträger, M., Schmitz, O.J., Gäb, S., Brockmann, K.J., Giese, R., Benter, T.: Atmospheric-pressure laser ionization: a novel ionization method for liquid chromatography/mass spectrometry. *Rapid Commun. Mass Spectrom.: RCM* **19**(3), 326–336 (2005)
- Davidson, P.A.: *Turbulence - an Introduction for Scientists and Engineers*. Oxford University Press, Oxford (2004)
- Derpmann, V., Kersten, H., Benter, T., Brockmann, K.J.: Ionisationsquelle und Verfahren zur Erzeugung von Analytionen. DE Patent 102011104709 A1, 2011
- Derpmann, V., Mueller, D., Bejan, I., Sonderfeld, H., Wilberscheid, S., Koppmann, R., Brockmann, K.J., Benter, T.: Capillary atmospheric pressure electron capture ionization (cAPECI): a highly efficient ionization method for nitroaromatic compounds. *J. Am. Soc. Mass Spectrom.* **25**(3), 329–342 (2014)
- Derpmann, V., Wißdorf, W., Müller, D., Benter, T.: Development of a New Ion Source for Capillary Atmospheric Pressure Electron Capture Ionization (cAPECI). Proceedings of the 60th ASMS Conference on Mass Spectrometry and Allied Topics, Vancouver (2012)
- Dimotakis, P.E.: Turbulent Mixing. *Annu. Rev. Fluid Mech.* **37**(1), 329–356 (2005)
- Eckhardt, B.: Introduction. Turbulence transition in pipe flow: 125th anniversary of the publication of Reynolds' paper. *Philos. Trans. R. Soc. A Math. Phys. Eng. Sci.* **367**(1888), 449–455 (2009)
- Eckhardt, B.: Applied physics. A critical point for turbulence. *Sci (New York, N.Y.)* **333**(6039), 165–166 (2011)
- Eckhardt, B., Schneider, T.M., Hof, B., Westerweel, J.: Turbulence transition in pipe flow. *Annu. Rev. Fluid Mech.* **39**(1), 447–468 (2007)

18. Eggels, J.G.M., Unger, F., Weiss, M.H., Westerweel, J., Adrian, R.J., Friedrich, R., Nieuwstadt, F.T.M.: Fully developed turbulent pipe flow: a comparison between direct numerical simulation and experiment. *J. Fluid Mech.* **268**(-1), 175 (1994)
19. Fomina, N.S., Kretinina, A.V., Masyukevich, S.V., Bulovich, S.V., Lapushkin, M.N., Gall, L.N., Gall, N.R.: Transport of ions and charged droplets from the atmospheric region into a gas dynamic interface. *Am. J. Anal. Chem.* **68**(13), 1151–1157 (2013)
20. Fox, R.W., McDonald, A.T., Pritchard, P.J.: *Introduction to Fluid Mechanics*, 6th edn. Wiley, Hoboken (2004)
21. N. Gimelshein, S. Gimelshein, T. Lilly, and E. Moskovets. Numerical Modeling of Ion Transport in an ESI-MS System. *J. Am. Soc. Mass Spectrom.* 820–831, 2014.
22. Hoge, H.J., Segars, R.A.: Choked flow - A generalization of the concept and some experimental data. *AIAA J.* **3**(12), 2177–2183 (1965)
23. H. Kersten. Development of an Atmospheric Pressure Ionization source for in situ monitoring of degradation products of atmospherically relevant volatile organic compounds. Dissertation, Bergische Universität Wuppertal, Germany, 2011.
24. Kersten, H., Brockmann, K.J., O'Brien, R., Benter, T.: Windowless Miniature Spark Discharge Light Sources for Efficient Generation of VUV Radiation Below 105 nm for On-Capillary APPI (CAPI). In: *Windowless Miniature Spark Discharge Light Sources for Efficient Generation of VUV Radiation Below 105 nm for On-Capillary APPI (CAPI)*. Proceedings of the 59th ASMS Conference on Mass Spectrometry and Allied Topics, Denver (2011)
25. Kersten, H., Derpmann, V., Barnes, I., Brockmann, K.J., O'Brien, R., Benter, T.: A novel APPI-MS setup for in situ degradation product studies of atmospherically relevant compounds: capillary atmospheric pressure photo ionization (cAPPI). *J. Am. Soc. Mass Spectrom.* **22**(11), 2070–2081 (2011)
26. Kersten, H., Wissdorf, W., Brockmann, K.J., Benter, T., O'Brien, R.: VUV Photoionization within Transfer Capillaries of Atmospheric Pressure Ionization Sources. Proceedings of the 58th ASMS Conference on Mass Spectrometry and Allied Topics, Salt Lake City (2010)
27. Klee, S., Derpmann, V., Kersten, H., Wißdorf, W., Müller, D., Brachthäuser, Y., Klopotoski, S., Brockmann, K.J., Benter, T.: Progress in the development of capillary Atmospheric Pressure Ionization Methods (cAPI). Proceedings of the 61st ASMS Conference on Mass Spectrometry and Allied Topics, Minneapolis (2013)
28. Klopotoski, S., Brachthäuser, Y., Mueller, D., Kersten, H., Wissdorf, W., Benter, T.: Characterization of API-MS Inlet Capillary Flow: Examination of Transfer Times and Choked Flow Conditions. Proceedings of the 60th ASMS Conference on Mass Spectrometry and Allied Topics, Vancouver (2012)
29. Klopotoski, S., Brachthäuser, Y., Müller, D., Kersten, H., Wissdorf, W., Derpmann, V., Brockmann, K.J., Janoske, U., Benter, T.: API-MS Transfer Capillary Flow: Examination of the Downstream Gas Expansion. Proceedings of the 59th ASMS Conference on Mass Spectrometry and Allied Topics, Denver (2011)
30. Laidler, K.J., Meiser, J.H.: *Physical Chemistry*. The Benjamin/Cummings Publishing Company, Inc., Menlo Park (1982)
31. Lin, B., Sunner, J.: Ion transport by viscous gas flow through capillaries. *J. Am. Soc. Mass Spectrom.* **5**(10), 873–885 (1994)
32. Livesey, R.G.: Solution methods for gas flow in ducts through the whole pressure regime. *Vacuum* **76**(1), 101–107 (2004)
33. Michalke, A.: Beitrag zur Rohrströmung kompressibler Fluide mit Reibung und Wärmeübergang. *Arch. Appl. Mech.* **57**(5), 377–392 (1987)
34. Reynolds, O.: An experimental investigation of the circumstances which determine whether the motion of water shall be direct or sinuous, and of the law of resistance in parallel channels. *Philos. Trans. R. Soc. Lond.* **174**, 935–982 (1883)
35. Reynolds, O.: On the dynamical theory of incompressible viscous fluids and the determination of the criterion. *Philos. Trans. R. Soc. A Math. Phys. Eng. Sci.* **186**, 123–164 (1895)
36. Santeler, D.J.: Exit loss in viscous tube flow. *J. Vac. Sci. Technol. A* **4**(3), 348 (1986)
37. Shapiro, A.H.: *The Dynamics and Thermodynamics of Compressible Fluid Flow*, volume 1. The Ronald Press Company, New York (1953)
38. Suter, S.P., Skalak, R.: The History of Poiseuille's Law. *Annu. Rev. Fluid Mech.* **25**(1), 1–20 (1993)
39. Sutherland, W.: LII. The viscosity of gases and molecular force. *Philos. Mag. Ser. 5* **36**(223), 507–531 (1893)
40. Taylor, G.: The dispersion of matter in turbulent flow through a pipe. *Pro. R.Soc.A: Math. Phys. Eng.Sci.* **223**(1155), 446–468 (1954)
41. Venerus, D.C.: Laminar capillary flow of compressible viscous fluids. *J. Fluid Mech.* **555**, 59 (2006)
42. Whitehouse, C.M., Dreyer, R.N., Yamashita, M., Fenn, J.B.: Electrospray interface for liquid chromatographs and mass spectrometers. *Anal. Chem.* **57**(3), 675–679 (1985)
43. Wutz, M., Adam, H.: *Theorie und Praxis der Vakuumtechnik*. Vieweg + Teubner Verlag, Braunschweig (1988)
44. Wutz, M., Adam, H., Walcher, W.: *Handbuch Vakuumtechnik*. Vieweg und Sohn Verlagsgesellschaft, Friedr, Braunschweig (1997)